J Therm Anal Calorim (2012) 107:127–134
DOI 10.1007/s10973-011-1548-z

Surfactant assisted preparation and characterization of carboxymethyl cellulose Sn(IV) phosphate composite nano-rod like cation exchanger

A thermodynamic study of pyridine adsorption

Ali Mohammad · Inamuddin · Arshi Amin

29th STAC-ICC Conference Special Chapter

Abstract Carboxymethyl cellulose Sn(IV) phosphate composite nano-rod like cation exchanger with diameter in the range of 20–40 nm, length in the range of 100–150 μm and particle size in the range of 21–38 nm have been successfully prepared by surfactant assisted sol–gel method. Scanning electron microscopy, transmission electron microscopy, X-ray powder diffraction, fourier transform infra red spectroscopy and thermogravimetric analysis-differential thermal analysis studies were carried out to study the structure and morphology of this composite nano-rod like cation exchanger. Freundlich adsorption isotherm is well fitted for the adsorption of pyridine on the surface of this composite nano-rod like cation exchanger. The thermodynamic parameters such as Freundlich constant, thermodynamic equilibrium constant (K_0), standard free energy changes (ΔG^0), standard enthalpy changes (ΔH^0) and standard entropy changes (ΔS^0) have been evaluated. These parameters indicated that the adsorption of pyridine on the surface of composite nano-rod like cation exchanger was feasible, spontaneous and exothermic in nature which suggests for the potential application of pyridine removal from water.

Keywords Composite nano-rod · Cation exchanger · Adsorption thermodynamics · Pyridine

A. Mohammad (✉) · Inamuddin · A. Amin
Department of Applied Chemistry, Faculty of Engineering and Technology, Aligarh Muslim University, Aligarh 202002, India
e-mail: alimohammad08@gmail.com

Introduction

Pyridine and its derivatives are being used as the most important intermediates in manufacturing of dyes, vitamins, pharmaceuticals, herbicides and insecticides as well as solvents for adhesives, varnishes and dye stuffs [1]. Consequently, pyridine and its derivatives are entering directly as industrial residue or indirectly as breakdown products of herbicides and insecticides into the environment. These are considered to be very toxic water pollutants even in very low concentration to aquatic life and human beings [2, 3]. Use of drinking water containing pyridine is causing persistent diseases like headache, nausea, giddiness, drowsiness, insomnia, increased heart rate, rapid breathing and liver damage in humans [4]. With the increasing concern of environment quality, rapid and efficient removal of pyridine and its derivatives from wastewater has drawn significant concern. Various methods such as biodegradation, photo-degradation, catalytic oxidation, liquid membrane separation and adsorption have been developed to remove pyridine from wastewater [5–7]. Among these methods, adsorption is one of the most attractive, cost effective, simple and widely used techniques for the treatment of wastewater. The adsorption process is primarily focused on the use of activated carbon as adsorbent, due to large surface area and predominant proportion of mesopores [8]. Nowadays, composite materials specially, nanomaterials are considered as alternatives to activated carbon for efficient removal of specific organics from contaminated wastewater, due to their large surface area and mechanical strength [9–17]. The adsorption properties of nanomaterials depend upon the particle size and surface morphology of composite. Controlling anisotropic behaviour of composite materials at the nanoscopic level is one of the most challenging issues for the

material scientists. In this study, composite nano-rod like cation exchanger having particle size in the range of 21–38 nm was prepared by sol–gel method. The composite nano-rod like cation exchanger was used as adsorbent to remove pyridine from wastewater and pyridine adsorption isotherm was studied.

Experimental

Reagents and chemicals

The main reagents viz stannic chloride, $SnCl_4 \cdot 5H_2O$ (95%), carboxymethyl cellulose sodium salt, *tri*-sodium orthophosphate dodecahydrate, $Na_3PO_4 \cdot 12H_2O$ (98%) and *N*-Cetyl-*N*,*N*,*N*-trimethyl ammonium bromide, $C_{19}H_{42}BrN$ (CTAB) (99%) used for the synthesis of the composite nano-rod like material were obtained from Central Drug House (CDH) Pvt. Ltd., India. Pyridine, C_5H_5N (99%) was obtained from E. Merck, India. The other reagents and chemicals used were of analytical reagent grade and used as received.

Instruments/apparatus used

A scanning electron microscope (SEM) (Leo 435 VP, Australia) and a transmission electron microscope (TEM) were used to examine the surface morphology and the particle size of the composite nano-rod like material.

An X-ray diffractometer (Phillips, Holland) model PW 1148/89 with Cu Kα radiations) was used to characterize the nature of composite nano-rod like material. A water bath incubator shaker (Narang Scientific Works Pvt. Ltd., India) having temperature variations of ±2 °C was used for all equilibrium studies. A digital pH meter (Elico LI-10, India) was used to adjust the pH of the solutions. A magnetic stirrer (Macro Scientific Works, India) was used for the mixing during the preparation of the composite nano-rod like material.

Fourier transform infra red (FTIR) spectroscopic spectra in the range 450–4500 cm^{-1} was recorded on FTIR spectrophotometer (Perkin Elmer spectrum-BX, USA). Thermogravimetric analyser (Perkin Elmer TGA) system of type TGA-7 was used to carry out thermogravimetric (TG) analysis of composite material in the temperature range from 60 to 870 °C at heating rate of 20 °C min^{-1}.

Experimental studies

Preparation of carboxymethyl cellulose Sn(IV) phosphate composite nano-rod like cation exchange material

In a typical preparation of composite nano-rod like cation exchanger, first of all Sn(IV) phosphate was prepared by mixing 0.1 M stannic chloride solutions prepared in 4 M HCl with aqueous solution of 0.1 M *tri*-sodium orthophosphate in different mixing volume ratios at room temperature (25 ± 2 °C). White precipitates of inorganic cation exchanger Sn(IV) phosphate were obtained, when pH of the solution was adjusted to 1 by adding aqueous ammonia/hydrochloric acid with constant stirring.

Further, 5 mL of CTAB was added in each precipitate of Sn(IV) phosphate. The precipitates of Sn(IV) phosphate so obtained were stirred for 10 min. Finally, 2 g of carboxymethyl cellulose sodium salt dissolved in 45 mL of demineralised water (DMW) was added in each precipitates of Sn(IV) phosphate. The resultant carboxymethyl cellulose Sn(IV) phosphate gels were stirred for 2 h using magnetic stirrer and kept for 24 h at room temperature (25 ± 2 °C) for digestion. At the final stage, the composite nano-rod like cation exchanger gels were filtered off by suction; washed with DMW to remove excess acid. The washed gels were dried over P_4O_{10} at 40 °C in an oven. The dried product was washed again with acetone to remove oligomers present in the material, and dried at 40 °C in an oven. The composite nano-rod like cation exchanger carries fixed phosphate ionic groups which are converted into H^+/counter ion form by treating with 1 M HNO_3 for 24 h with occasional shaking and intermittently replacing the supernatant liquid with fresh acid 2–3 times. The excess acid was removed after several washings with DMW and finally dried at 50 °C. The composite nano-rod like cation exchanger was cracked and the particle size of approximately 125 μm was obtained by sieving and stored in desiccator. The ion exchange capacity was determined by standard column process. For this purpose, 1 g of the dry cation exchanger samples in the H^+-forms were taken into different glass columns having an internal diameter (i.d.) ~1 cm and fitted with glass wool support at the bottom. The bed length was approximately 1.5 cm long. 1 M $NaNO_3$ as eluent was used to elute the H^+ ions completely from the cation exchange columns, maintaining a very slow flow rate (~0.5 mL min^{-1}). The effluents were titrated against a standard 0.1 M NaOH solution for the total ions liberated in the solutions using phenolphthalein indicator and the ion exchange capacities in meq dry g^{-1} are determined. The conditions of the preparation, the ion exchange capacity and the physical appearances of the organic, inorganic and composite cation exchangers are given in Table 1.

Adsorption equilibrium and thermodynamics study

Batch technique was selected to study the equilibrium and thermodynamics for the adsorption of pyridine onto the surface of carboxymethyl cellulose Sn(IV) phosphate composite nano-rod like cation exchange material (S-5).

Table 1 Conditions for the preparation of carboxymethyl cellulose Sn(IV) phosphate composite nano-rod like cation exchanger

Samples	Mixing volume ratio (V/V)			Carboxymethyl cellulose sodium salt added/g	Colour of beads obtained after drying	Na^+ ion exchange capacity/meq dry g^{-1}
	0.1 M $SnCl_4 \cdot 5H_2O$ in 4 M HCl	0.1 M $Na_3PO_4 \cdot 12H_2O$	pH			
1	1	0.5	1	2	White	1.09
2	1	1	1	2	White	1.69
3	1	1.5	1	2	White	1.91
4	1	2	1	–	White	1.20
5	1	2	1	2	White	2.13
6	1	3	1	2	White	1.95
7	1	4	1	2	White	2.01

Stock solution of pyridine was prepared by dissolving 0.1 N of pyridine in distilled water. The solution was further diluted to get desired concentration. A 0.5 g of carboxymethyl cellulose Sn(IV) phosphate composite nano-rod like cation exchanger were added in various stoppered conical flasks, each containing 20 mL of pyridine solutions of different concentrations ranging from 2.5×10^{-3} to 15×10^{-3} N at three different desired temperatures viz 35, 50 and 65 °C. The equilibrium time was measured at different contact duration ranged between 2 and 24 h and a fixed temperature 25 °C. It was observed that the equilibrium was achieved after 6 h of agitation as shown in Fig. 1. Therefore, the mixtures were shaken for 6 h, each to attain equilibrium. The composite nano-rod like cation exchange material was filtered off and the supernatant liquid for the residual concentration of pyridine was analysed titrimetrically [18]. Initial concentrations of pyridine prior to composite nano-rod like cation exchanger mixing were also analysed similarly.

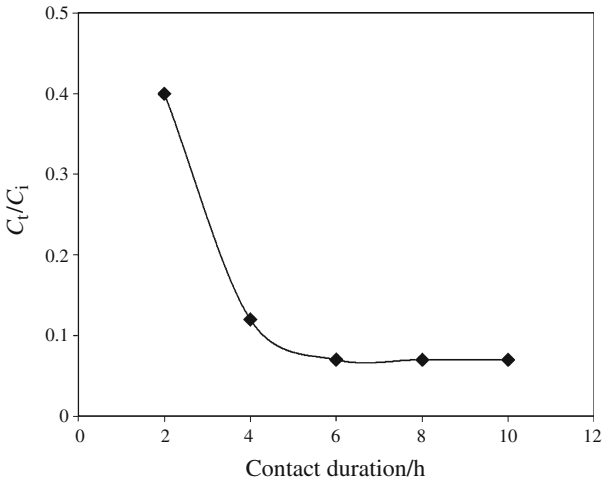

Fig. 1 A plot of time versus the ratio between the pyridine concentration at a given moment (C_t) and initial pyridine concentration (C_i) for the determination of infinite time of exchange

Results and discussion

Various samples of carboxymethyl cellulose Sn(IV) phosphate composite nano-rod like cation exchanger were successfully prepared via surfactant assisted sol–gel method. In a typical sol–gel process, CTAB was mixed with white inorganic precipitate of Sn(IV) phosphate followed by the addition of carboxymethyl cellulose at room temperature. The condition of preparation and ion exchange capacity is given in Table 1. The ion exchange capacity of composite nano-rod like cation exchanger was found to be higher (2.13 meq dry g^{-1}) as compared to the ion exchange capacity of inorganic ion exchanger Sn(IV) phosphate (1.2 meq dry g^{-1}). The observed increase in exchange capacity is considered due to the binding of organic polymer with inorganic moiety. The attractive feature of this cation exchanger is the creation of organic–inorganic composite nano-rod like morphology during binding of organic polymer with inorganic precipitates which enhances the ion exchange capacity and contributes towards the better adsorption of pyridine chosen in this study.

Surface morphology and particle size of composite carboxymethyl cellulose Sn(IV) phosphate powder (S-5), observed from scanning electron microscopy and transmission electron microscopy are represented in Figs. 2 and 3, respectively.

Figure 2 a and b shows SEM images at low and high magnifications of carboxymethyl cellulose Sn(IV) phosphate (S-5). It is clear from the SEM images that the prepared composite consists of nano-rod like morphology with a diameter in the range of 20–40 nm and length in the range of 100–150 μm. It can also be seen from TEM images of composite in Fig. 3 that as-prepared composite consist of low scale nano-particles of size in the range of 21–38 nm.

The X-ray powder diffraction pattern of composite nano-rod like cation exchanger (S-5) is represented in

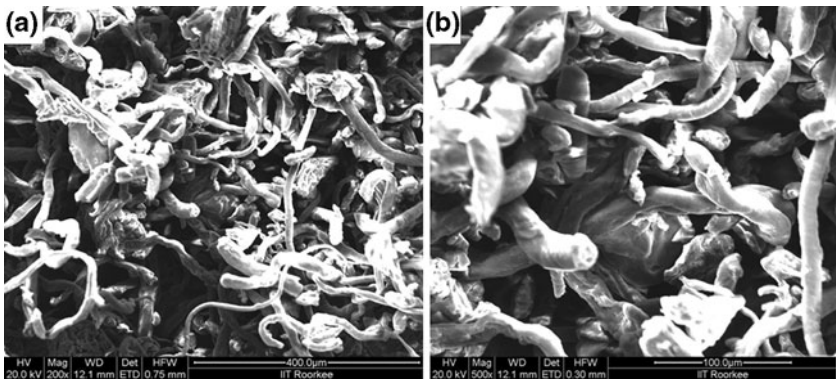

Fig. 2 SEM images at low (**a**) and high (**b**) magnifications of the carboxymethyl cellulose Sn(IV) phosphate composite nano-rod like cation exchanger

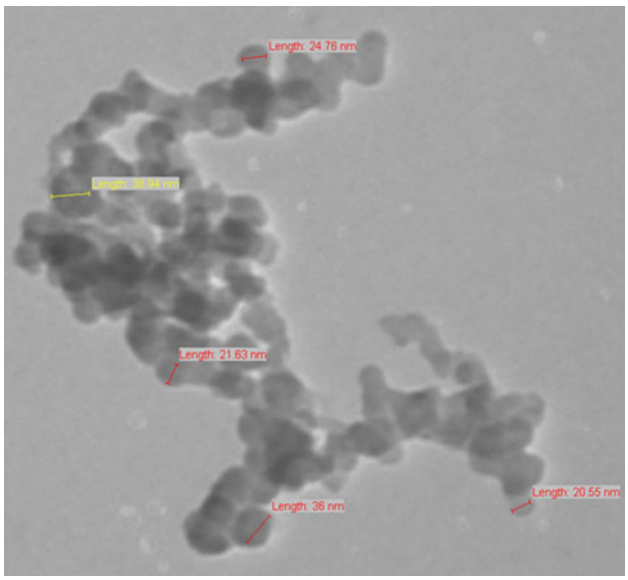

Fig. 3 TEM image of the carboxymethyl cellulose Sn(IV) phosphate composite nano-rod like cation exchanger

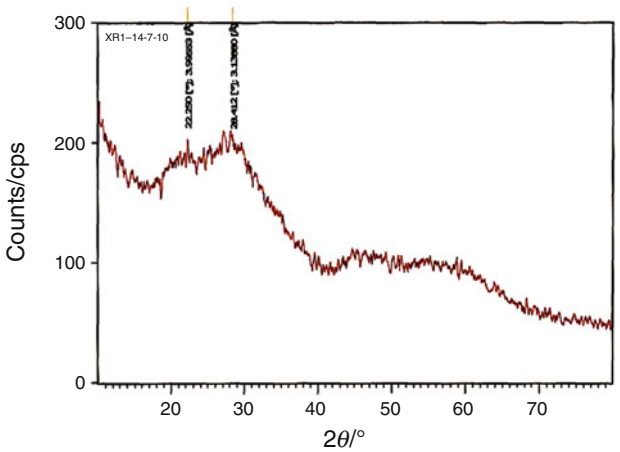

Fig. 4 Powder X-ray diffraction pattern of carboxymethyl cellulose Sn(IV) phosphate composite nano-rod like cation exchanger

Fig. 4, which showed very small peaks of 2θ values. The analysis of these small signal peaks supports its semi-crystalline nature. In addition, the wide peaks indicate the average crystalline size of the composite nano-rod like cation exchanger [19].

Fourier transform infra red spectrum of as prepared carboxymethyl cellulose Sn(IV) phosphate composite nano-rod like cation exchanger (S-5) is shown in Fig. 5. It is evident from FTIR spectrum that composite nano-rod like cation exchanger shows the characteristic absorption peaks attributed to the presence of organic polymers carboxymethyl cellulose, external water molecule and metal oxygen bonds of Sn(IV) phosphate.

In the spectrum of composite material, the broad absorption peak at 3411 cm^{-1} corresponds to the stretching vibrations of hydroxyl (–OH) groups [20]. Basically, the –OH groups represent the presence of absorbed water and secondary alcohols groups. The broadness of the peaks may be assigned due to the presence of intermolecular and intra-molecular hydrogen bonds [21]. The sharp absorption band around 1633 cm^{-1} confirms the presence of –COO groups. The band around 1403 cm^{-1} is assigned to $–CH_2$ scissoring, while the band around 1057 cm^{-1} is ascribed due to the presence of $CHO–CH_2$ stretching [20] as well as ionic phosphate groups [22]. An assembly of two sharp peaks in the region of 619–533 cm^{-1} may be due to the presence of metal oxygen bond [23].

From the TG curve of this composite cation exchanger shown in Fig. 6, it is observed that the loss of mass (about 8%) up to 138.3 °C may be due to the removal of external water molecule present at the surface of the material [24, p. 315]. A slow mass loss of (∼7%) is observed in between 138.3 and 255.6 °C may be due to the removal of interstitial water molecules removed by condensation of –OH groups together with external water molecules from the materials. A mass loss of (∼9.02%) is observed in between 255.6 and 357.4 °C may be due to the condensation of phosphate to pyrophosphate groups [24, p. 330]. Further, mass loss of (∼5.6%) between 357.4 and 620 °C may be due to complete decomposition of organic part of the composite material. From 620 °C onwards, a smooth horizontal section represents the complex formation of oxide

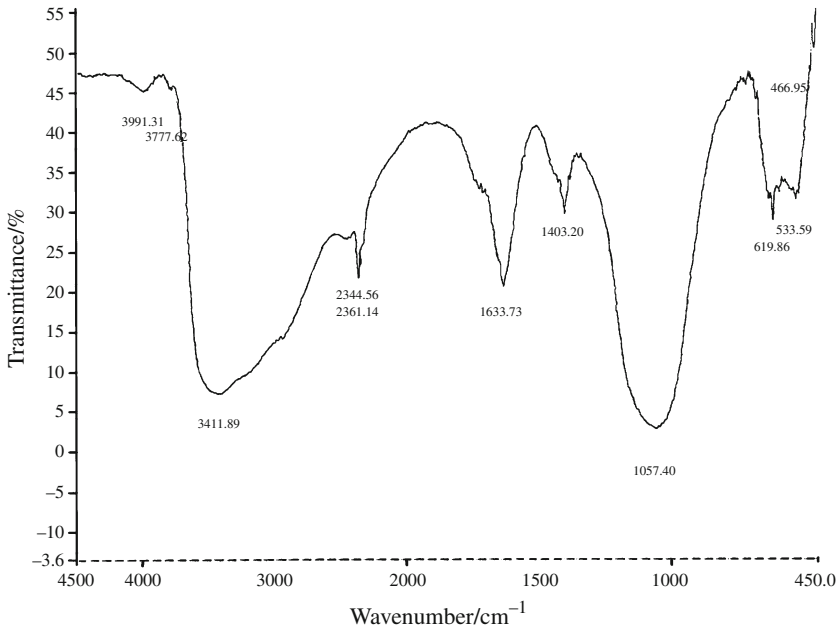

Fig. 5 FTIR spectrum of carboxymethyl cellulose Sn(IV) phosphate composite nano-rod like cation exchanger

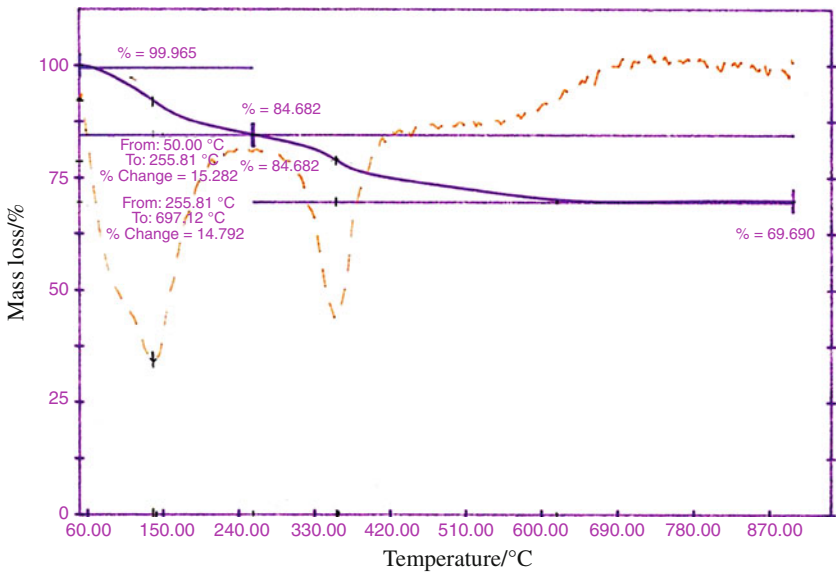

Fig. 6 TG–DTA analysis of carboxymethyl cellulose Sn(IV) phosphate composite nano-rod like cation exchanger

from the material. The total mass loss of (~30.01%) is comparatively lower than other composite materials of this class, which indicates towards the better thermal stability of this composite cation exchanger. The structural transformations observed by TG analysis have also been supported by differential thermal analysis (DTA). The DTA curve showed two exothermic peaks with maxima at 138 and 357 °C that confirm the structural transformations in the composite nano-rod like cation exchanger.

Freundlich adsorption isotherm for the adsorption of aqueous pyridine on the solid surface of carboxymethyl cellulose Sn(IV) phosphate composite nano-rod like cation exchanger at three different temperatures viz 35, 50 and 65 °C was used to understand the mechanism of adsorption of pyridine and quantifying the distribution of pyridine in aqueous phase and the solid cation exchanger phase at equilibrium during the adsorption process. The adsorption isotherms are shown in Fig. 7. All isotherms follow adequately Freundlich adsorption behaviour and can be represented by the equation:

$$x/m = KC^{1/n} \quad (1)$$

where x/m is the surface concentration of pyridine in millimoles per gram of the cation exchanger represented as C_s, C is the equilibrium concentration of pyridine (m mol mL^{-1}) represented as C_e. According to this equation, plots of log C_s versus log C_e are straight lines at all three temperatures seen in Fig. 7 and K and $1/n$ are the

constants determined from the intercepts and slopes of the starting lines, respectively, fitted to the points by the least squares method. The values obtained are listed in Table 2. The values of *1/n* are lying between 0 and 1 confirm the favourable conditions for the adsorption of pyridine [25]. It was observed that the values of K are decreasing with increasing temperature suggesting the exothermic process of pyridine adsorption [26]. The values of K and *1/n* are the measure of pyridine adsorption capacity and adsorption intensity, respectively. The applicability of Freundlich adsorption isotherm for the adsorption of pyridine on the solid surface of composite nano-rod like cation exchanger is confirmed by the higher value of regression coefficient, R.

Thermodynamic parameters were calculated from the variation of the thermodynamic equilibrium constant K_0 (or sorption distribution coefficient) with the change in temperature. The constant, K_0 for the adsorption reaction can be defined as follows:

$$K_0 = \frac{a_s}{a_e} = \frac{v_s\, C_s}{v_s\, C_e} \tag{2}$$

where a_s is the activity of adsorbed solute, a_e is the activity of the solute in solution at equilibrium, C_s is the surface concentration of pyridine in m mol per gram of exchanger, C_e is the concentration of pyridine at equilibrium (m mol mL^{-1}), v_s is the activity coefficient of the adsorbed solute and v_e is the activity coefficient of the solute in solution.

As the concentration of the solute in the solution approaches zero, the activity coefficient approaches unity, reducing Eq. 2 to the following form:

$$K_0 = \frac{a_s}{a_e} = \frac{C_s}{C_e} \tag{3}$$

The values of sorption distribution coefficient K_0 are determined by plotting ln (C_s/C_e) versus C_s at different temperatures (Fig. 8) and extrapolating C_s to zero [27]. The straight line obtained is fitted to the points based on a least squares analysis. Its intercept with the vertical axis gives the values of K_0. Standard free energy changes (ΔG^0) for interactions using the sorption distribution coefficient (K_0) are calculated from the relationship given below [28].

$$\Delta G^0 = -RT \ln K_0 \tag{4}$$

where R is the universal gas constant and T is the temperature in Kelvin. The average standard enthalpy change (ΔH^0) is then calculated from the well-known Van't Hoff equation:

$$\ln K_0(T_3) - \ln K_0(T_1) = \frac{-\Delta H^0\ (T_1 \text{ to } T_3)}{R}\left(\frac{1}{T_3} - \frac{1}{T_1}\right) \tag{5}$$

where T_3 and T_1 are two different temperatures. Standard entropy changes (ΔS^0) are calculated using the equation:

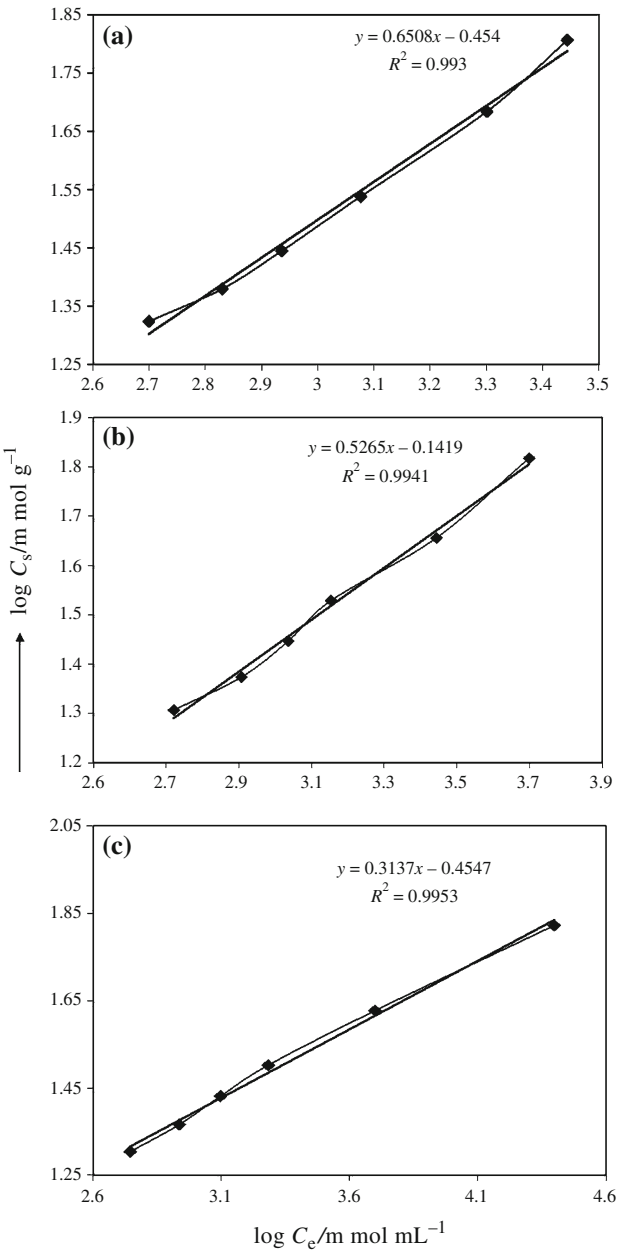

Fig. 7 Freundlich adsorption isotherms of pyridine adsorption at temperatures 35 °C (**a**), 50 °C (**b**) and 65 °C (**c**) on carboxymethyl cellulose Sn(IV) phosphate composite nano-rod like cation exchanger

Table 2 Freundlich isotherm constants K and *1/n* for the adsorption of pyridine on carboxymethyl cellulose Sn(IV) phosphate composite nano-rod like cation exchanger

Freundlich constant	Temperature/°C		
	35	50	65
K	0.454	0.141	0.454
1/n	0.650	0.526	0.313
R^2	0.993	0.994	0.995

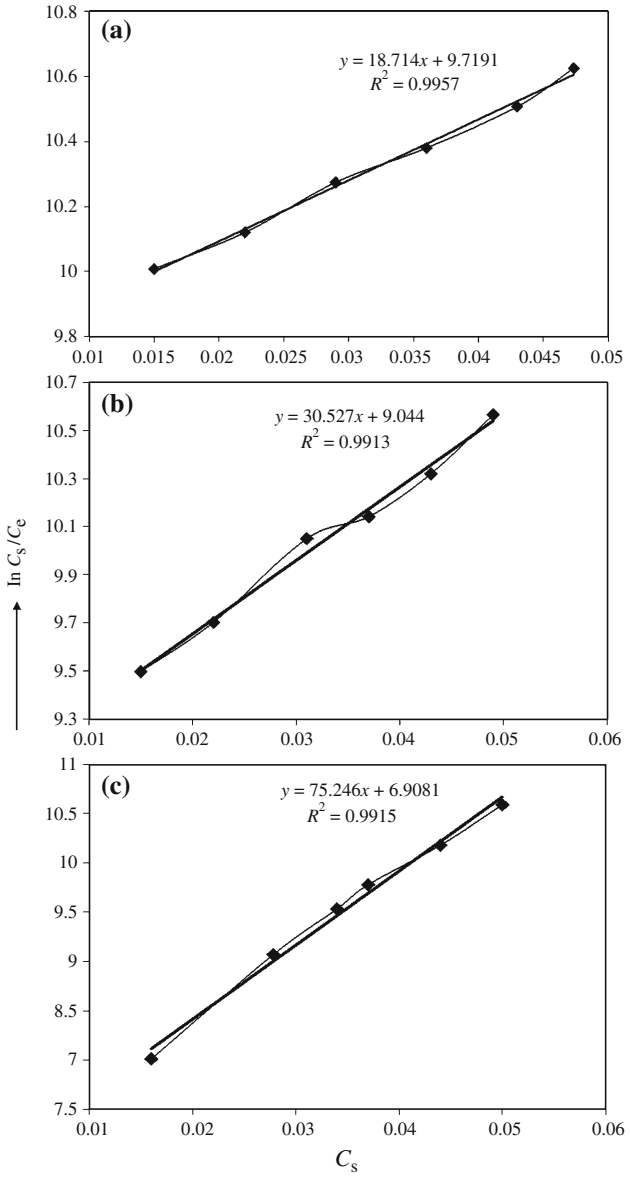

Fig. 8 Plots of ln C_s/C_e versus C_s at temperatures 35 °C (**a**), 50 °C (**b**) and 65 °C (**c**) on carboxymethyl cellulose Sn(IV) phosphate composite nano-rod like cation exchanger

$$\Delta G^0 = \Delta H^0 - T\Delta S^0 \quad (6)$$

The values of Gibbs free energy, ΔG^0 (kcal mol^{-1}); enthalpy, ΔH^0 (kcal mol^{-1}) and entropy, ΔS^0 (kcal mol^{-1} deg^{-1}) observed for the adsorption process of pyridine on the surface of composite nano-rod like are given in Table 3.

The negative values of Gibbs free energy, ΔG^0 indicated the spontaneous process of pyridine adsorption at 35, 50 and 65 °C. The negative values of standard enthalpy change (ΔH^0) indicated that the pyridine-exchanger interaction during adsorption process is favoured by heat given off; as an exothermic reaction. Hence, the adsorption of pyridine was favoured at lower temperature and molecules of pyridine were orderly adsorbed on the surface of composite nano-rod like cation exchanger. Since the free energy as well as enthalpy changes are negative and accompanied by increased (positive) entropy changes (ΔS^0), the reactions are spontaneous and exothermic with a high affinity for pyridine.

Table 3 Values of various thermodynamic parameters for the adsorption of pyridine on carboxymethyl cellulose Sn(IV) phosphate composite nano-rod like cation exchanger

Thermodynamic constant	Temperature/°C		
	35	50	65
K_0	9.719	9.044	6.908
ΔG^0/kcal mol^{-1}	−1.3921	−1.4136	−1.298
ΔH^0/kcal mol^{-1}	−2.35192	−2.35192	−2.35192
ΔS^0/kcal mol^{-1}deg^{-1}	1.215×10^{-3}	1.166×10^{-3}	1.080×10^{-3}

Conclusions

In this study, carboxymethyl cellulose Sn(IV) phosphate composite nano-rod like cation exchanger was prepared by sol–gel process. The composite nano-rod like cation exchanger was characterized to observe the structure, surface morphology and particle size. The adsorption of pyridine on the solid surface of composite nano-rod like cation exchanger followed Freundlich adsorption isotherm. Adsorption process is driven by decreasing enthalpy i.e. liberation of heat (exothermic process) or negative (ΔH^0) and negative free energy change (ΔG^0), i.e. adsorption process is spontaneous while the increase in entropy (positive ΔS^0) indicated the increased disorder during the adsorption process. This composite nano-rod like cation exchanger may be utilized for the removal of pyridine from aqueous solutions due to efficient adsorption process.

Acknowledgements The authors are thankful to Department of Applied Chemistry, Z. H. College of Engineering and Technology, A.M.U. (Aligarh) for providing research facilities and also to the University Grants Commission, New Delhi (India) for financial assistance.

References

1. Ramos RL, Perez RO, Rivera OLT, Mendoza MSB, Castillo NAM. Kinetics of pyridine adsorption onto granular activated carbon. J Basic Princ Diffus Theory Exp Appl. 2009;11:1–2.
2. Henry GD. De novo synthesis of substituted pyridines. Tetrahedron. 2004;60:6043–61.
3. Yanli Z, Dongguang L. Adsorption of pyridine on post-cross-linked fiber. J Sci Ind Res. 2010;69:73–6.
4. U.S. Environmental Protection Agency. Toxic Substance Control Act. Washington, DC;1979.

5. Herrmann JM. Heterogeneous photocatalysis: fundamentals and applications to the removal of various types of aqueous pollutants. Catal Today. 1999;53:115–29.
6. Drijvers D, Langenhove HV, Bechers MW. Decomposition of phenol and trichloroethylene by the ultrasound/H_2O_2/CuO process. Water Res. 1998;33:1187–94.
7. Zhao B, Liang HD, Han DM, Qiu D, Chen SQ. Adsorption of pyridine from aqueous solution by surface treated carbon nanotubes. Sep Sci Technol. 2007;42:3419–27.
8. Lataye DH, Mishra IM, Mall ID. Removal of pyridine from liquid and gas phase by copper forms of natural and synthetic zeolites. Ind Eng Chem Res. 2006;45:3934–43.
9. Mojumdar SC, Raki L. Preparation and properties of calcium silicate hydrate-poly (vinyl alcohol) nanocomposite materials. J Therm Anal Calorim. 2005;82:89–95.
10. Mukherjee GS. Calorimetric characterization of membrane materials based on polyvinyl alcohol. J Therm Anal Calorim. 2009;96(1):21–5.
11. Bittencourt PRS, Santos GLD, Pineda EAG, Hechenleitner. Studies on the thermal stability and film irradiation effect of poly (vinyl alcohol)/Kraft lignin blends. J Therm Anal Calorim. 2005;79:371–4.
12. Cuiying L, Wei Z, Bo Z, Mei L, Canhui L. Preparation, characterization and thermal behaviour of poly(vinyl alcohol)/organic montmorillonite nanocomposites through solid-state shear pan-milling. J Therm Anal Calorim. 2011;103(1):205–12.
13. Vlase G, Vlase T, Doca N, Perta M, Ilia G, Plesu N. Thermal behaviour of a sol-gel system containing aniline and organic phosphonates. J Therm Anal Calorim. 2009;97:473–8.
14. Nabi SA, Bushra R, Naushad M, Khan AM. Synthesis, characterization and analytical applications of a new composite cation exchange material poly-*o*-toluidine stannic molybdate for the separation of toxic metal ions. Chem Eng J. 2010;165(2):529–36.
15. Nabi SA, Bushra R, Al-Othman ZA, Naushad M. Synthesis, characterization and analytical applications of a new composite cation exchange material acetonitrile stannic(IV) selenite: Adsorption behaviour of toxic metal ions in non-ionic surfactant medium. Sep Sci Technol. 2011;46. doi: 10.1080/01496395.2010.534759 (in press).
16. Al-Othman ZA, Inamuddin NM. Determination of ion-exchange kinetic parameters for the poly-o-methoxyaniline Zr(IV) molybdate composite cation-exchanger. Chem Eng J. 2011;166(2):639–45.
17. Al-Othman ZA, Inamuddin, Naushad M. Adsorption thermodynamics of trichloroacetic acid herbicide on polypyrrole Th(IV) phosphate composite cation-exchanger. Chem. Engg. J. 2011;46. doi: 10.1016/j.cej.2011.02.046 (in press).
18. Qureshi M, Varshney KG, Alam KZ, Ahmad A. Adsorption of tertiary nitrogen-containing compounds on activated carbon. II. Equilibrium studies of 2, 6-lutidine in aqueous system. Colloid Surf. 1990;50:17–24.
19. Zhu G, Liu P, Hojamberdiev M, Zhou JP, Huang X, Feng B, Yang R. Controllable synthesis of PbI_2 nanocrystals via a surfactant-assisted hydrothermal route. Appl Phys A. 2010;98:299–304.
20. Hebeish A, Higazy A, El-Shafei A, Sharaf S. Synthesis of carboxymethyl cellulose (CMC) and starch-based hybrids and their applications in flocculation and sizing. Carbohydr Polym. 2010;79:60–9.
21. Ibrahim AA, Adel AM, El-Wahab ZHA, Al-Shemy MT. Utilization of carboxymethyl cellulose based on bean hulls as chelating agent. Synthesis, characterization and biological activity. Carbohydr Polym. 2011;83:94–115.
22. Rao CNR. Chemical applications of infrared spectroscopy. New York: Academic Press; 1963. p. 338.
23. Liang S, Teng F, Bulgan G, Zong R, Zhu Y. Effect of phase structure of MnO_2 nanorod catalyst on the activity for CO oxidation. J Phys Chem C. 2008;112:5307–15.
24. Duval C. Inorganic thermogravimetric analysis. Amsterdam: Elsevier; 1963.
25. Sundaram CS, Viswanathan N, Meenakshi S. Fluoride sorption by nano-hydroxyapatite/chitin composite. J Hazard Mater. 2009;172:147–51.
26. Zhu HY, Jiang R, Xiao L, Zeng GM. Preparation, characterization, adsorption kinetics and thermodynamics of novel magnetic chitosan enwrapping nanosized γ-Fe2O3 and multi-walled carbon nanotubes with enhanced adsorption properties for methyl orange. Bioresour Technol. 2010;101:63.
27. Biggar JW, Cheung MW. Adsorption of picloram (4-amino-3,5,6-trichloropicolinic acid) on Panoche, Ephrata, and Palouse soils: a thermodynamic approach to the adsorption mechanism. Soil Sci Soc Am J. 1973;37:863–8.
28. Glasstone S. Text book of physical chemistry. New York: Van Nostrand; 1960. p. 815.